SECOND EUROPEAN CONFERENCE ON EARTHQUAKE ENGINEERING
AND SEISMOLOGY, ISTANBUL AUG. 25-29, 2014

NORMAL FAULT INDUCED GROUND DEFORMATIONS AND THE ASSOCIATED BENDING RESPONSE OF BURIED PIPELINES

Pengpeng NI[1], Ian D. MOORE[2] and W. Andy TAKE[3]

ABSTRACT

In order to cover wide geographic areas, it is inevitable that pipelines must pass through unfavourable ground conditions which are susceptible to natural disasters. Beam-on-spring analysis is the normal design approach for evaluating pipeline response across ground faults. Winkler model models the soil medium as a series of independent elastic-perfectly-plastic springs acting in parallel along the pipe. This assumption cannot capture the interaction through the soil from one location to the next and becomes invalid when large ground distortion induces second order effects for the beam-type structure or gaps are generated at the soil-pipe interface. Recent experimental and numerical studies show that design codes are not capable of producing the required soil-pipe interaction force versus deformation relationships. The nature of soil-structure interaction for pipelines has been further investigated to develop an appropriate design method. This paper presents a parametric study using the three-dimensional finite element approach to evaluate the effects of diameter, burial and bedding depth, and the effect of the pipe and soil properties on the pipe's flexural responses. The numerical results are compared with calculations obtained using a new set of approximate design equations. This study can also help in choosing dimensions for large-scale tests of the normal fault-pipeline interaction problem.

INTRODUCTION

When an earthquake strikes, unexpected permanent ground movement can be induced. These large soil distortions may exert detrimental effects on buried pipelines. Seismic demands on buried pipelines due to bedrock faulting need to be estimated, against which capacity can be compared. The pipe design in terms of burial depth, pipe material, Standard Dimension Ratio (the ratio of pipe diameter to wall thickness), backfill soil and its compaction can then be determined that minimizes the potential risk of failure or leakage.

Beam-on-spring analysis is the normal design approach for these soil-pipeline interaction problems as specified in current design guidelines such as ASCE (1984). It is known that designs based on these independent simplified bilinear soil springs are problematic, and may lead to overconservative or unconservative estimation of the demand. Ha and his colleagues conducted a series of centrifuge model tests to evaluate the soil-pipe interaction force versus deformation relationship (i.e. the p-y relationship) (Ha et al., 2008). They found that the test gave a result consistent with the ASCE guidelines for strike-slip faulting, but the measured p-y relationship for normal faulting is much lower than the ASCE relationship for the side having upward soil movements. Using Ha's centrifuge data, numerical analysis using the Winkler-type model produced good agreement with the test results when a factor of 1/6 was employed to reduce the ultimate strength of the vertical soil

[1] Ph.D. candidate, Queen's University, Kingston, Canada, e-mail address: pengpeng.ni@ce.queensu.ca
[2] Professor, Queen's University, Kingston, Canada, e-mail address: moore@civil.queensu.ca
[3] Associate Professor, Queen's University, Kingston, Canada, e-mail address: andy.take@civil.queensu.ca

springs resisting downward deformation (Xie et al., 2013). Some pipe pullout tests indicate that design codes tend to over- and under-estimate axial resistance applied to pipes in loose and dense sand, respectively (Weerasekara and Wijewickreme, 2008). Other analytical models reported in the literature (Karamitros et al., 2007; Kennedy et al., 1977; Newmark and Hall, 1975) all feature complex interactions which hinder their application by practical engineers. A better understanding of the physical phenomena and a new simplified design method capturing the soil-structure interaction for buried pipelines under differential ground movement are needed.

This paper presents a three-dimensional finite element analysis of the normal fault-pipeline interaction problem. Earlier work by the authors demonstrated the effectiveness of a continuum modelling strategy against centrifuge test data (Saiyar, 2011), and incorporated both numerical simulations and centrifuge test results to develop a set of approximate equations for preliminary design estimates of longitudinal moments associated with normal faulting (Ni et al., 2014). A parametric study is here reported which systematically addresses the effects of model scale (via pipe diameter, burial depth, and bedding depth), stress level (via burial depth), bedding depth to burial depth ratio, and the sensitivity to the pipe and soil properties. Calculations of the peak pipe curvature using the simplified design method of Ni et al. (2014) are compared with the numerical results for three different configurations. The minimum pipeline test length is calculated using twice the distance from inflection point to where curvature vanishes to guide the selection of test dimensions for large-scale geotechnical tests of normal fault-pipeline interaction being planned in the GeoEngineering Laboratory at Queen's University (Moore, 2013).

PARAMETRIC ANALYSIS PLAN

The buried pipeline within a uniform soil deposit straddling a normal fault with a dip angle of 90° is portrayed in Fig. 1. A pipe at a burial depth H sits at a bedding depth BD above the underlying rock stratum, where the normal fault offset (δ_0) at the hanging wall side is generated. The seismic waves were found to reduce the shear strength of the surrounding soil, and so reduce the pipe strains (Sim et al., 2012). It is reasonable to make the test easier by defining an upper bound deformation, where a relatively slow quasi-static process associated with an abrupt fault rupture is applied (Bransby et al., 2007).

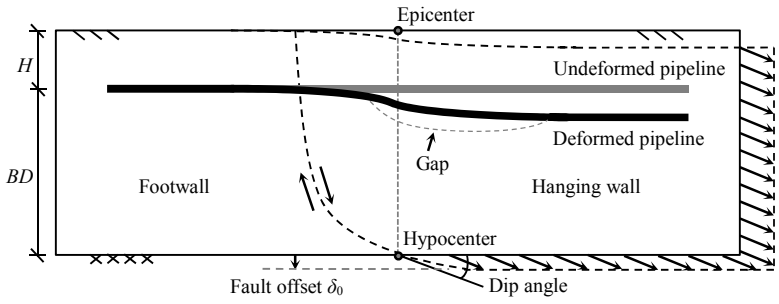

Figure 1. Definition and geometry of the problem

Two pipe materials and three types of soil are used to investigate the effect of relative pipe-soil stiffness on pipe behaviour. Following the earlier work (Ni et al., 2014), a solid rod approximation is employed in the analysis to represent the thin-walled tube prototype pipe under increased gravity (30 g) environment. All geometries are scaled down 30 times in the analysis. In this paper, all results are presented in the prototype-based scale, unless otherwise stated.

The properties of the two pipes are listed in Table 1, where D is the pipe diameter, t is the thickness, I is the moment of inertia, E is the Young's modulus, P is the allowable internal pressure, and the subscripts p and s represent the pipe and solid rod, respectively. HDPE pipe has the density of 0.95 g/cm^3 and Poisson's ratio of 0.4. Modulus of elasticity for HDPE pipe is highly time dependent and chosen as 350 MPa here according to its one-week response (Moore and Hu, 1996). For steel pipe, the typical characteristics are selected as follows: density of 7.9 g/cm^3, Poisson's ratio of 0.3 and modulus of elasticity of 200 GPa.

Table 1. Pipe material properties

Pipe	Thin-walled tube prototype pipe						Solid rod centrifuge pipe				
	D (m)	t (mm)	I_p (m^4)	E_p (GPa)	E_pI_p ($MN{\cdot}m^2$)	P (MPa)	D (m)	I_p, I_s (m^4)	E_p (MPa)	E_pI_p ($MN{\cdot}m^2$)	E_p* (GPa)
HDPE	0.12	12.7	6.25E-6	0.35	2.19E-3	1.72	0.12	1.02E-5	214.82	2.19E-3	0.23
	0.24	30	1.11E-4	0.35	3.90E-2	1.72	0.24	1.63E-4	239.26	3.90E-2	0.23
	0.48	56.4	1.71E-3	0.35	6.00E-1	1.72	0.48	2.61E-3	230.13	6.00E-1	0.23
Steel	0.12	6.4	3.70E-6	200	7.39E-1	53.6	0.12	1.02E-5	72625.01	7.39E-1	71
	0.24	12	5.60E-5	200	1.12E+1	47.4	0.24	1.63E-4	68780.00	1.12E+1	71
	0.48	25.4	9.40E-4	200	1.88E+2	52.9	0.48	2.61E-3	72149.07	1.88E+2	71

* The model characteristics are simplified by using a single value of modulus for all the three pipe diameters

Fraser River sand at relative densities of 69% and then 100% (FRS69 and FRS100) are used to represent coarse-grained backfill in loose and dense compaction conditions, respectively (as tested triaxially at appropriate, low confining pressure by Karimian (2006)). In addition, sandy silt backfill at 85% standard Proctor density (ML85) is included as a third soil option (Selig, 1990). Using the Janbu (1963) approach, initial tangent modulus (E_{ini}) is estimated as a power function of the initially isotropic effective confining stress σ_3' (a hyperelastic approximation), Fig. 2. In particular,

$$E_{ini} = K_i p_a \left(\frac{\sigma_3'}{p_a} \right)^n \tag{1}$$

where K_i is a dimensionless "modulus number", P_a is the atmospheric pressure (with the same units as σ_3'), and n is a dimensionless "modulus exponent" that determines the rate of variation of E_{ini} with σ_3'.

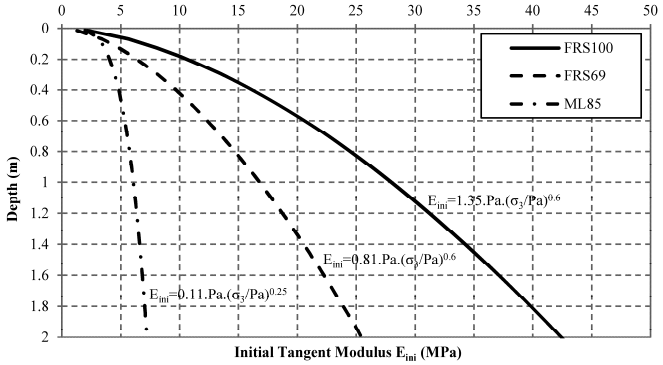

Figure 2. Initial tangent modulus varying with depth

Table 2. Summary of numerical models

Model name	D (m)	H (m)	H/D	BD (m)	BD/H	δ_0 (m)
M1	0.24	0.6	2.5	3	5	0.21
M2	0.24	1.2	5	3	2.5	0.21
M3	0.24	1.8	7.5	3	1.67	0.21
M4	0.12	0.6	5	6	10	0.105
M5	0.12	1.2	10	6	5	0.105
M6	0.12	1.8	15	6	3.33	0.105
M7	0.24	0.6	2.5	6	10	0.21
M8	0.24	1.2	5	6	5	0.21
M9	0.24	1.8	7.5	6	3.33	0.21
M10	0.48	0.6	1.25	6	10	0.42
M11	0.48	1.2	2.5	6	5	0.42
M12	0.48	1.8	3.75	6	3.33	0.42
M13	0.24	0.6	2.5	9	15	0.21
M14	0.24	1.2	5	9	7.5	0.21
M15	0.24	1.8	7.5	9	5	0.21

Table 2 is a summary of the parameters for each numerical model, where the H/D ratio falls within the range from 1 to 10 suggested by the ASCE (1984) guideline. The imposed fault offset δ_0 is restricted to $0.5D$ given that localized buckling occurs when faulting increases up to $0.7D$ level in the strike-slip fault-pipeline interaction analysis performed by Vazouras et al. (2010). This choice considers that the design framework developed by Ni et al. (2014) is based on thin beam theory and only applicable to pipe response working in the elastic range. For each model, six configurations are considered, involving the two pipe materials and the three different backfills. Table 3 gives the range of relative pipe-soil stiffness for all the studied cases. In total, results from 90 analyses are presented.

Table 3. Relative pipe-soil stiffness

Soil	H (m)	E_s (MPa)	HDPE pipe		Steel pipe	
			E_p (MPa)	E_pI_p/E_sI_s	E_p (MPa)	E_pI_p/E_sI_s
FRS100	0.6	4.27	230	54	71000	16620
	1.2	6.50	230	35	71000	10931
	1.8	8.29	230	28	71000	8564
FRS69	0.6	2.56	230	90	71000	27700
	1.2	3.90	230	59	71000	18218
	1.8	4.97	230	46	71000	14274
ML85	0.6	1.40	230	164	71000	50687
	1.2	1.68	230	137	71000	42182
	1.8	1.87	230	123	71000	38002

FINITE ELEMENT METHOD SETUP

Parametric analyses were conducted using three-dimensional continuum modelling in ABAQUS/Explicit. Energy dissipation then has to be checked to reproduce a quasi-static process of fault propagation. To minimize the kinetic energy and eliminate the inertia effect, a sufficiently slow loading rate was employed.

The large discontinuity across the faulting zone was imposed using a ramp function, where the underlying rock fault is spread across a narrow zone instead of applying an abrupt deformation to the finite elements immediately above the fault. The width of this narrow zone (r) has to coincide with the physical behaviour of strain localization within the brittle soils (Muir Wood, 2002). A typical mesh (that for the model denoted M9) is shown in Fig. 3, where fine elements are used near the fault and coarse elements are employed at the pipe ends. Shear deformation due to faulting only affects a small portion of soil, and the induced bending response of pipe will vanish after a certain length.

Half the pipe is modelled using eight-node hexahedral continuum elements with elastic material properties. Under low confining pressure, the surrounding soil is characterized by the conventional Mohr-Coulomb model, with constant friction angle capable of reproducing the pipe response under lateral soil motion observed in tests (Robert, 2010; Yimsiri et al., 2004). Further modelling of strain softening phenomena is not feasible for this parametric analysis. However, in reality, soil stiffness and strength varies with the level of effective confining stress, with different soil properties employed at different depths. A fraction (1/3) of the initial modulus is used to calculate the secant modulus to correctly estimate the elastic response of the soil (Karimian, 2006). The peak friction angles (φ_p) of three soils (FRS100, FRS69 and ML85) fall within the range of 52°-49°, 47°-44° and 42°-38° (high friction angle at low confining pressure). Fraser River sand has a constant volume internal friction angle (φ_{cv}) of 34°, while φ_{cv} is evaluated as 30° for ML85. Cohesion has been determined as 3 kPa and 20 kPa for Fraser River sand and ML85 and Poisson's ratio of 0.3 and 0.24 respectively (Karimian, 2006; Selig, 1990). The soil-pipe interface is modelled using the contact surface approach wherein slip and separation is allowed to occur between the two surfaces. The interface friction coefficient μ is tentatively selected as 0.3, since this value has little impact on the flexural response of the pipe (Vazouras et al., 2010). For further details of the numerical modelling, the reader is referred to Ni et al. (2014).

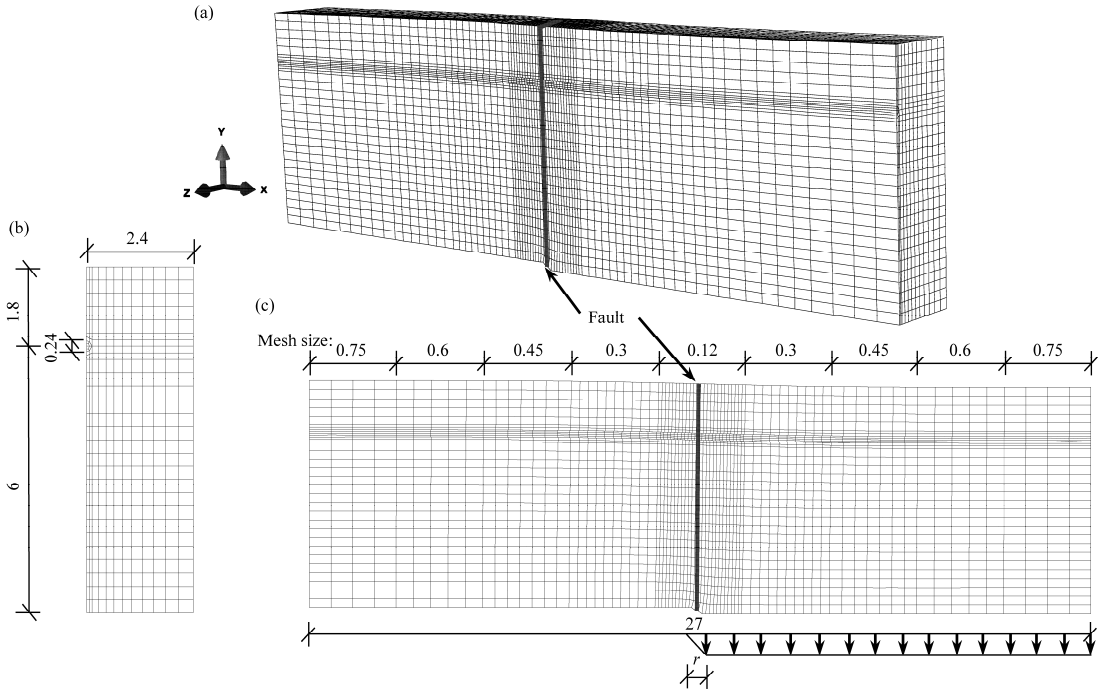

Figure 3. Finite element discretization of the (a) soil formation with tectonic fault, (b) cross-section and (c) elevation view with ramp function

ANALYSIS AND DISCUSSION OF RESULTS

Deflection profiles for the soil and pipe are normalized against imposed fault level δ_0 and shown in Fig. 4a. Before localized buckling occurs, the pipe is assumed to deform in the elastic range. The fault is applied with dislocations rising up to half the pipe diameter, so that shear deformations of the pipe cross-section can be ignored. The pipe follows Timoshenko's plane cross-section assumption and its length is more than 20 times the diameter. Therefore, thin beam theory can be used to derive the flexural response quantified by bending curvature (Fig. 4b), from deflection profiles using double differentiation. The critical location along the pipe (x) of concern in design is the location of peak pipe curvature ($\kappa_{\max}$), which is denoted i (i_{pipe}: pipe profile in pipe tests and i_{soil}: soil profile at pipe elevation in free field tests). This quantity provides the distance from the location of pipe peak curvature to the point of contraflexure (x_c).

When a pipe straddles a normal fault, the responses of pipe sections in both the footwall and hanging wall sides are different. This non-symmetric behaviour is induced by different soil-structure interaction forces exerted along the pipe. The pipe deforms in the hogging mode at the footwall side, which causes upward soil-structure interaction forces on the pipe. This is analogous to soil response during bearing failure under strip footings. On the hanging wall side, however, the pipe deforms in sagging and lifts the soil up. The applied soil-structure interaction forces then correspond to the pull-out capacity for anchor plates. The two mechanisms differ, in that the bearing capacity of the soil is greater than its uplift counterpart (O'Rourke and Liu, 1999). Higher bending moments and associated curvatures can then occur in the hogging zone. Meanwhile, this large magnitude of curvature spreads a shorter distance, which is reflected by lower values of i_{pipe} and i_{soil} (Ni et al., 2014). Design using larger pipe peak curvature $\kappa_{\max}$ and smaller i_{pipe} is then conservative. Therefore, parameters in the hogging zone will be reported hereafter.

Free field tests with no pipe included are conducted for three backfill materials. The information regarding shear band, strain localization and fault rupture propagation through the soil are then be gathered. The value of i_{soil}, independent of fault offset δ_0, indicates how soil deformation patterns spread at a given depth (Ni et al., 2014). For each soil type, 9 configurations of soil layer thickness t_{soil} have been evaluated where the ratio between bedding depth BD to burial depth H varies. In Fig. 5, the

variations of i_{soil} as a function of depth from the ground surface are shown for soil materials FRS100 and ML85. The hollow markers represent the data points obtained from the numerical simulations, and straight lines give best fit lines for these data that can be used for design purposes. Bilinear approximations of i_{soil} versus depth shed light on the extent of plastic responses developed within the soil due to the displacement discontinuity induced by faulting. Highly concentrated shear strains are expected at greater depths (near the base rock), where soil responds in the plastic range. Less dislocation of the elements occurs near the ground surface. At a certain depth, the dominant soil behaviour alters from plastic to elastic (with a corresponding change of slope seen in Fig. 5). The depth ratio H/t_{soil} determines the degrees of ground discontinuity and consequently the soil-structure interaction forces if a pipe is buried within.

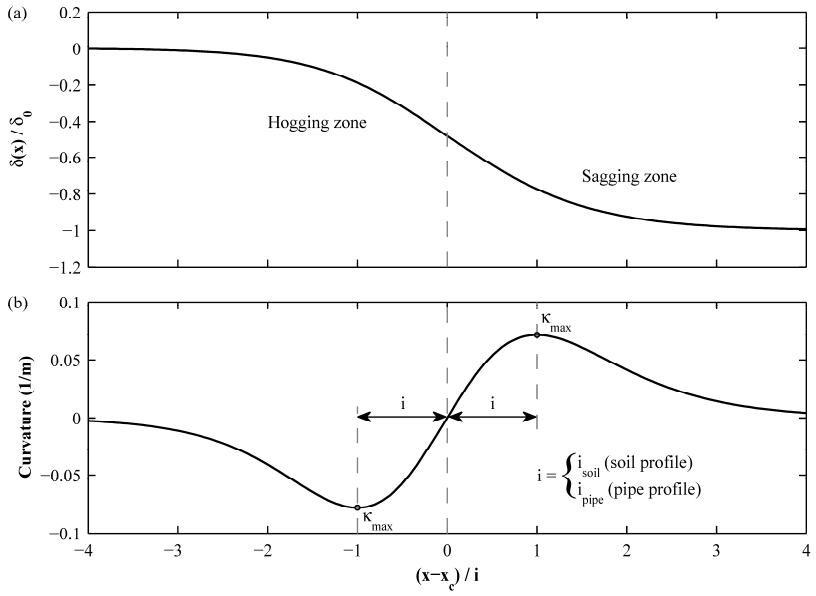

Figure 4. Examples of M3 model: (a) deflection and (b) curvature profiles of soil (FRS69) and pipe (HDPE)

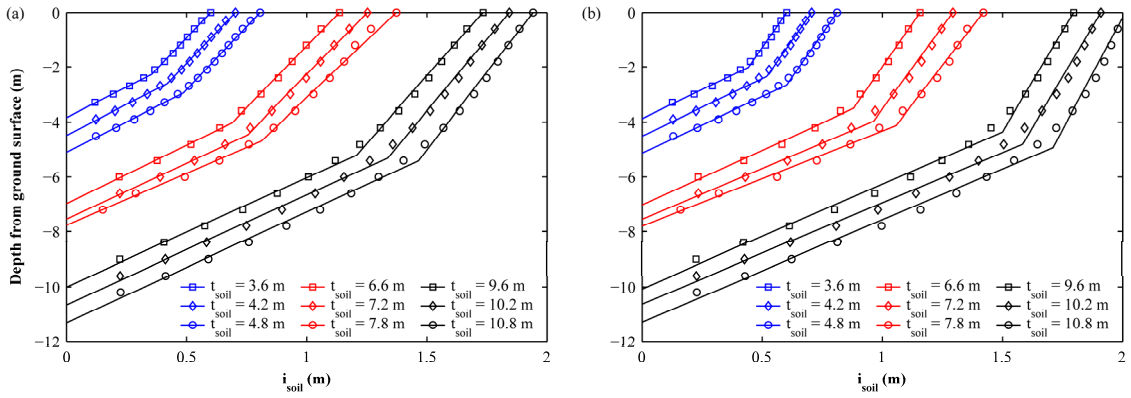

Figure 5. Variation of i_{soil} with depth from ground surface: (a) FRS 100 and (b) ML85

For a specific problem geometry (pipe diameter, burial depth and bedding depth), the effect of soil properties on flexural pipe responses has also been investigated. Fig. 6 presents three model examples, where the values of i_{pipe} and pipe peak curvature κ_{max} are compared for different backfill materials. As expected, i_{pipe} is almost independent of fault level δ_0. An approximately linear relationship between κ_{max} with δ_0 supports the interpretation that the pipe is responding in the elastic range. Steel pipe has larger i_{pipe} and smaller κ_{max} values than HDPE pipe, since the stiff pipe bridges more effectively across the shear zone, which changes the fault propagation path, as well as the deformation profile of the pipe. The fault rupture appears to avoid the buried structure and the shear

deformations are spreading more extensively along the pipe. The stronger and stiffer backfill material (FRS100) leads to smaller relative pipe-soil stiffness, which is the cause of the more concentrated pipe responses (shorter i_{pipe} and higher κ_{max}). Although the strength parameters vary significantly for FRS100 and FRS69, there is negligible effect on pipe responses. Compared with Fraser River sand, ML85 has a lower Poisson's ratio, which produces larger i_{pipe} and smaller κ_{max} values. Soil dilates when it experiences shear, which influences the strength and deformation behaviour of granular soils. Dilation angle controls the volume expansion (deformation), however, it is more directly related to shear strength degradation. The only kinematic parameter defined here is Poisson's ratio, which is believed to result in the difference in pipe responses for different backfill materials.

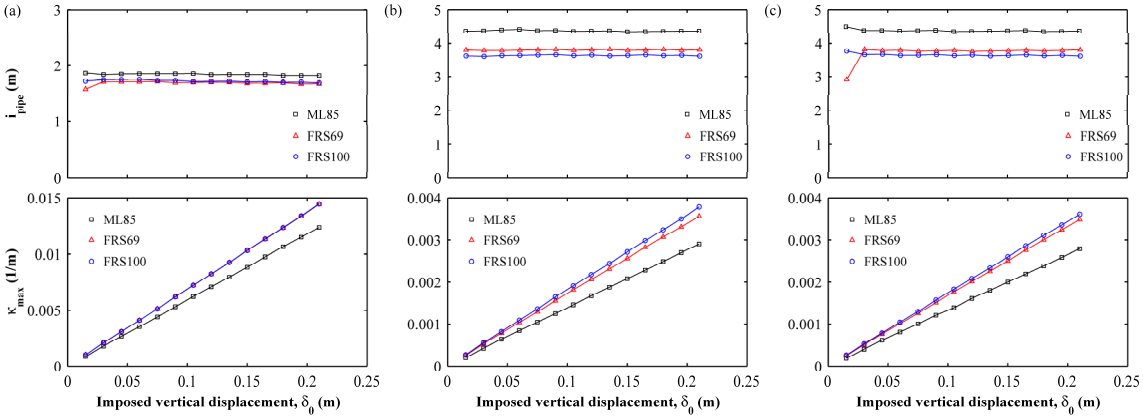

Figure 6. The effect of backfill soils on pipe responses: (a) M12 model, HDPE pipe, (b) M4 model, steel pipe and (c) M8 model, steel pipe

The scale effect of pipe diameter on flexural response is studied and the comparisons are presented in Fig. 7. A base analysis can be selected as the pipe test with diameter of 0.24 m, against which parametric analyses obtained using different diameters can be compared, while all other model scales are kept consistent. All pipes are loaded up to a faulting level corresponding to half a pipe diameter. Three models with different diameters produce almost identical results (the only difference is the level of fault dislocation imposed, since this was set to half the pipe diameter). Hence, diameter could be neglected in the following analysis and only the pipe models with the 0.24 m diameter will be presented hereafter.

The results illustrated in Fig. 8 show the influence of bedding depth to burial depth ratio on pipe flexural responses. A constant ratio BD/H of 5 results in significantly different values of i_{pipe} and κ_{max}. There is an approximately proportional relationship between i_{pipe} and depths H or BD. On the other hand, κ_{max} is inversely proportional to depths H or BD. To investigate which depth contributes most to the response variations, analyses using varying burial depth H and bedding depth BD are performed and presented in Figs. 9 and 10, respectively. It is clear that stress level (via burial depth) alters the responses much less than bedding depth does. The increase of overburden pressure (more soil above the pipe, Fig. 9) corresponds to more restraint imposed on the pipe, which in turn helps to reduce the peak curvature and to spread curvatures further along the structure. This effect becomes less notable when steel pipe is included that the change in relative pipe-soil stiffness induced by adding the burial stress is small. As an interpretation of the parametric analyses of bedding depth in Fig. 10, one can infer that increases in the soil between the base rock and the pipe leads to larger soil layer thickness where the fault propagates before reaching and influencing on the pipe. With smaller bedding depth, greater displacement discontinuity is expected at the elevation of the pipe. This causes large soil-structure interaction forces and consequently severe peak pipe curvature κ_{max}. These curvatures develop within a short distance (i_{pipe} is small), which is detrimental to the pipe. From a practical point of view, pipes should be buried far away from the base rock stratum and have large burial depth, given that the pipe wall is designed strong enough to withstand the increased overburden pressure. If the scenario is a site with a very shallow soil layer above the base rock, pipes should be laid near the ground surface due to the greater influence of bedding depth rather than burial depth on the pipe's flexural response.

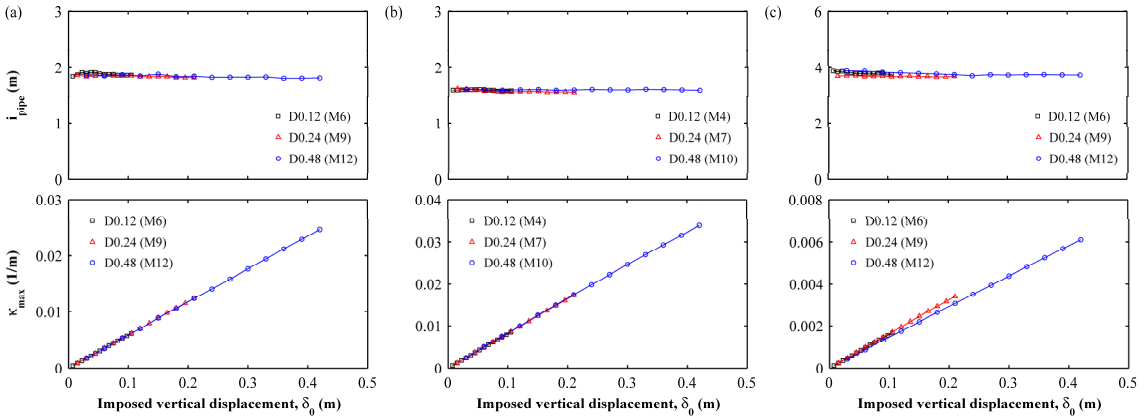

Figure 7. The effect of diameter *D* on pipe responses: (a) HDPE pipe buried in ML85, (b) HDPE pipe buried in FRS69 and (c) Steel pipe buried in FRS100

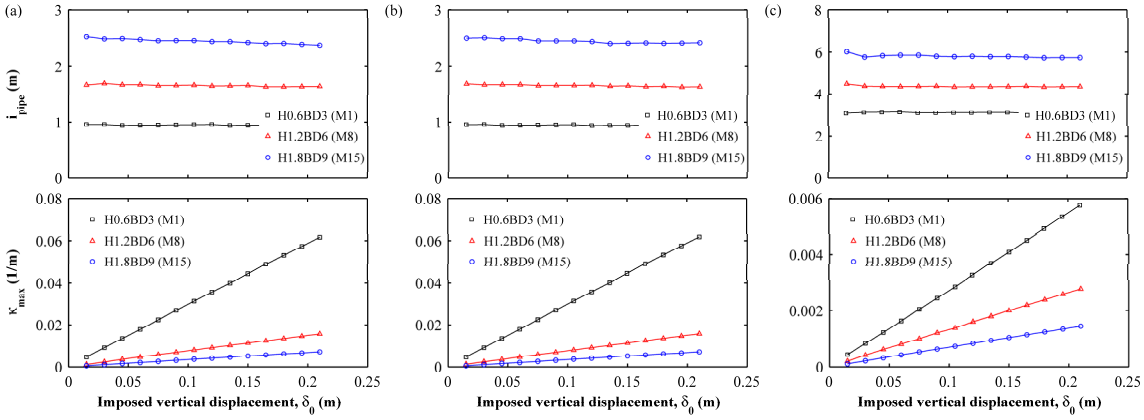

Figure 8. The effect of *BD*/*H* ratio on pipe responses: (a) HDPE pipe buried in FRS69, (b) HDPE pipe buried in FRS100 and (c) Steel pipe buried in ML85

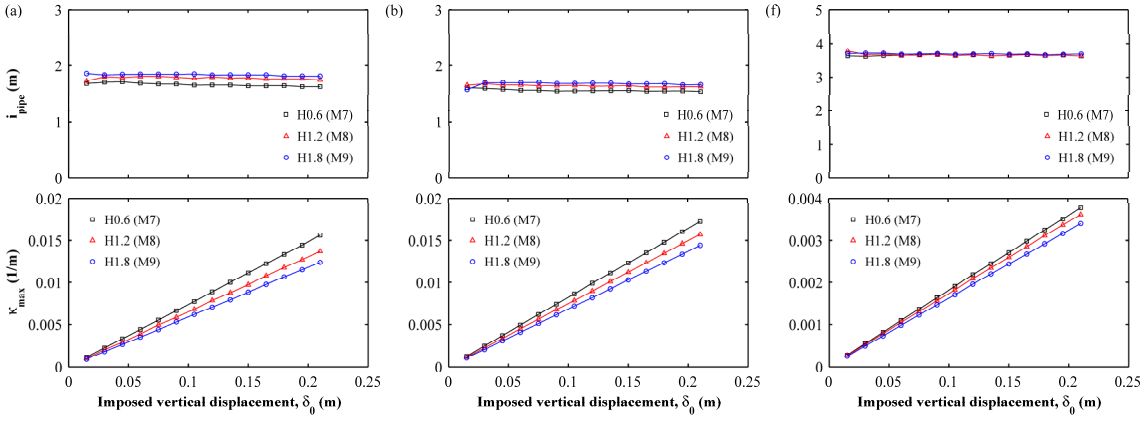

Figure 9. The effect of burial depth *H* on pipe responses: (a) HDPE pipe buried in ML85, (b) HDPE pipe buried in FRS69 and (c) Steel pipe buried in FRS100

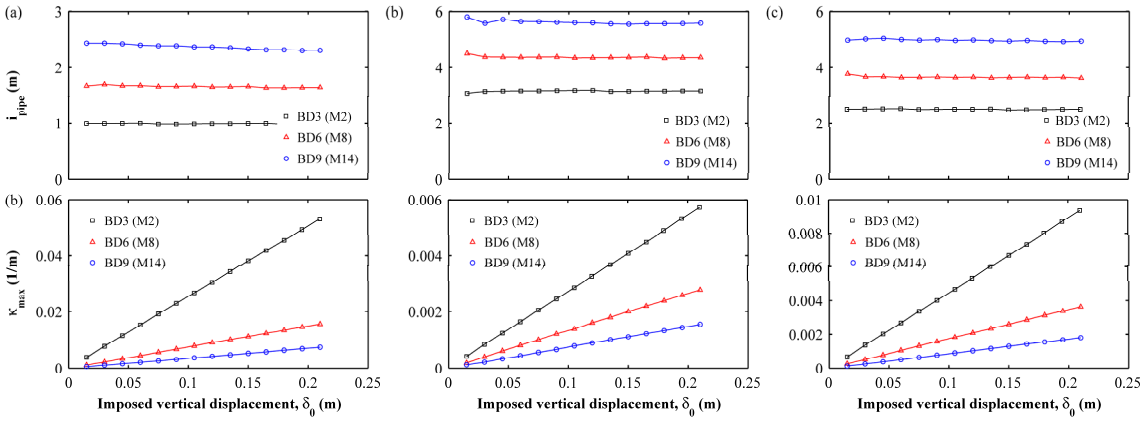

Figure 10. The effect of bedding depth *BD* on pipe responses: (a) HDPE pipe buried in FRS69, (b) Steel pipe buried in ML85 and (c) Steel pipe buried in FRS100

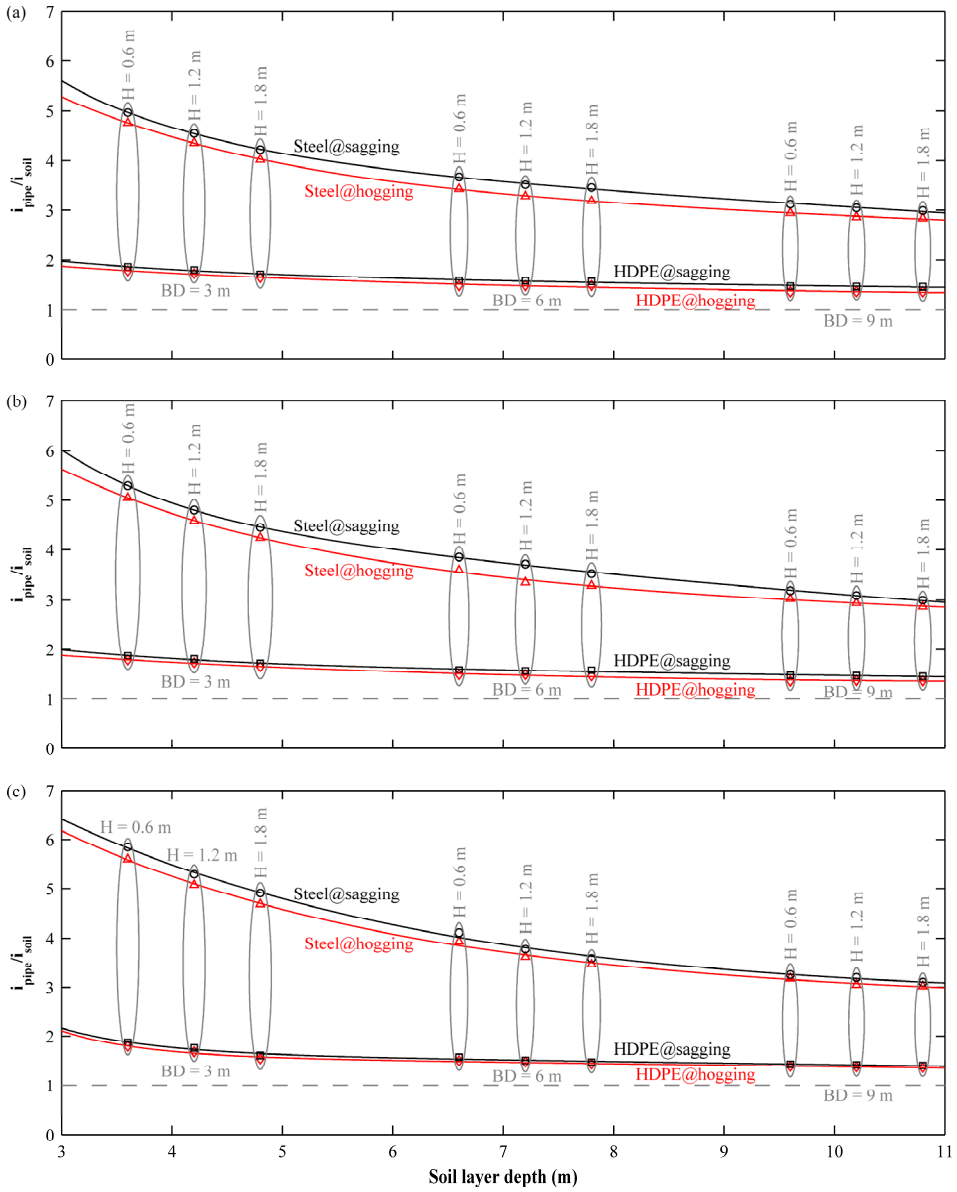

Figure 11. Ratio of i_{pipe}/i_{soil} varying with soil layer depth t_{soil}: (a) FRS 100, (b) FRS69 and (c) ML85

Both i_{soil} and i_{pipe} are almost independent of imposed fault offset δ_0 (Ni et al., 2014), and the averaged values can be considered as an inherent property once a burial configuration (pipe and soil properties, burial and bedding depths) is determined. Incorporating all data from the 54 base analyses (pipe diameter of 0.24 m), the relationships between i_{pipe}/i_{soil} ratio and soil layer thickness t_{soil} are exhibited in Fig. 11. Numerical results and the approximate power function calculations are shown using hollow markers and lines respectively. The pipe sections respond differently in the sagging and hogging zones. However, this difference is modest for both pipes. The differences in the ratio i_{pipe}/i_{soil} evaluated in the sagging and hogging zones are 6.1%, 6.1%, and 3.5% for HDPE pipe buried in FRS100, FRS69 and ML85, respectively. For steel pipe, these values correspond to 6.0%, 6.1% and 4.0%. Use of results in the hogging zone could lead to a conservative design (smaller i_{pipe} and larger κ_{max}). HDPE pipe has small relative pipe-soil stiffness, and it complies (moves in phase) with the soil deformations (i_{pipe}/i_{soil} is close to 1). The effect of higher steel pipe stiffness and its additional bridging across the ground fault results in more noticeable shear band dispersion and larger value for i_{pipe}/i_{soil}. In Figs. 11a, 11b to 11c, the ratio i_{pipe}/i_{soil} increases slightly when the soil modulus reduces from FRS100, to FRS69, and to ML85. This coincides with the observation in Fig. 6 that increased relative pipe-soil stiffness produces larger i_{pipe} and smaller κ_{max}. However, the pipe's flexural responses are not very sensitive to the soil properties, and much more closely related to burial depth H and especially bedding depth BD.

When pipes are designed for areas prone to differential ground motion, structural engineers need to evaluate the maximum bending moment (or curvature). A new design framework has been proposed that provides curvatures at the 16th and 84th percentiles, corresponding to one standard deviation from the mean (50th percentile) of all centrifuge (Saiyar, 2011) and numerical data, as representative of lower and upper bounds of pipe peak curvature (Ni et al., 2014).

$$\left| \frac{\kappa_{max} i_{pipe}^{\ 2}}{\delta_0} \right|_{16th} = 0.239 \tag{2}$$

$$\left| \frac{\kappa_{max} i_{pipe}^{\ 2}}{\delta_0} \right|_{84th} = 0.326 \tag{3}$$

Correct estimate of the i_{pipe} value is then crucial to derive the pipe peak curvature from these two expressions. Three calculation examples are tabulated in Table 4, along with the numerical results. Fitting functions give reasonable evaluations of i_{pipe} compared with numerical data, which differ by 1.0%, 1.8% and 3.6% from the M1, M9 and M14 model calculations respectively. The value of i_{pipe} can also indicate the required length scale for use in large-scale geotechnical tests of normal fault-pipeline interaction, like those being planned in the GeoEngineering Laboratory at Queen's University (Moore, 2013). For example, when an HDPE pipe is laid at a buried depth of 0.6 m and a bedding depth of 1.2 m in ML85 soil, the required length is approximately 4 m (four times the i_{pipe} value). The comparisons of the pipe peak curvature obtained through numerical simulations and the simplified design method of Ni et al. (2014) are presented in Fig. 12. All these three case studies show that the numerical data falls within the range of the lower (16th percentile) and upper (84th percentile) bound calculations.

Table 4. Calculations of i_{pipe} from i_{soil}

Model	Pipe	Soil	i_{soil} (m) from Fig. 5		i_{pipe}/i_{soil} from Fig. 11		i_{pipe} (m)	
			Numerical data	Bilinear fit	Numerical data	Power fit	Numerical data	Calculations
M1	HDPE	ML85	0.56	0.53	1.79	1.95	1.04	1.03
M9	Steel	FRS69	1.16	1.19	3.29	3.25	3.81	3.88
M14	Steel	ML85	1.84	1.83	3.05	3.18	5.62	5.82

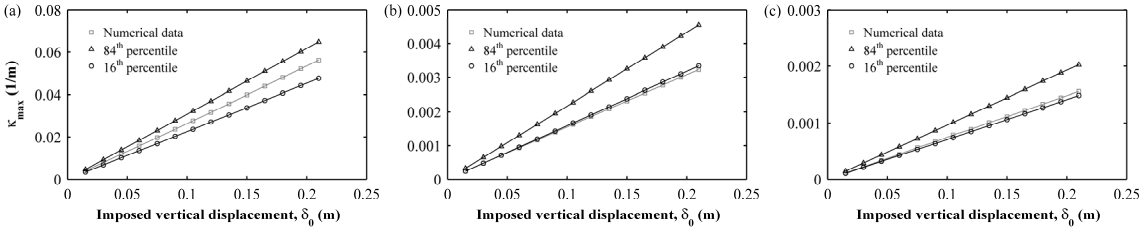

Figure 12. Comparison of peak curvatures: (a) M1 model, HDPE pipe buried in ML85, (b) M9 model, Steel pipe buried in FRS69 and (c) M14 model, Steel pipe buried in ML85

CONCLUSIONS

The response of continuous pipe have been studied for intersection at 90° with a normal fault with dip angle of 90°. Flexural response is dominant and axial soil-structure interaction forces can generally be neglected. The authors have previously reported the success of finite element analyses of centrifuge tests, and the current study evaluates the influence of parameters such as pipe diameter, burial depth, bedding depth, and the sensitivity to the pipe and soil properties.

Fault offsets with magnitudes of up to half a pipe diameter were imposed, where the pipe response remains within the elastic range. Hence, thin beam theory can be used to compute the curvature distributions through direct differentiation of the deformation profile of the pipe. The distance from the location of the point of contraflexure (at or near the concentrated shear zone that develops in the soil) and the point of peak curvature (κ_{max}) is denoted as i_{soil} for soil response in a free field condition (without a pipe present), and i_{pipe} quantifies this distance along the pipe. A bilinear approximation was found to reasonably represent the variations of i_{soil} with depth from the ground surface for use in evaluating i_{soil} at the pipe elevation. Almost identical values of i_{pipe} and κ_{max} are obtained for varying pipe diameters. The influence of backfill materials and burial depths on pipe response is negligible compared with bedding depth. Use of stiff soil decreases the relative pipe-soil stiffness, so that larger κ_{max} and smaller i_{pipe} result. The increase of both burial and bedding depths helps to introduce more soil restraint to the pipe and reduces the flexural responses (smaller κ_{max} and larger i_{pipe}). Stiffness of the pipe determines to what extent the pipe bridges across the underlying soil, with steel pipe spreading deformations more than HDPE pipe. In practice, pipes should be placed as far as possible from the bedrock to avoid the severe displacement discontinuity when a fault occurs.

The effectiveness of the approximate design equations proposed (Ni et al., 2014) has been evaluated through comparisons of the pipe peak curvatures obtained from numerical results and the simplified design calculations. This method can serve as a first approximation for the peak longitudinal bending moments during design. The calculated i_{pipe} value also provides guidance for the selection of test dimensions for large-scale geotechnical tests of normal fault-pipeline interaction being planned in the GeoEngineering Laboratory at Queen's University (Moore, 2013). Full-scale tests can be used to evaluate the efficacy of both the centrifuge tests on small-scale model pipes and the numerical analysis. These tests may also assist in building confidence in the efficacy of the new design framework.

REFERENCES

ASCE (1984) Guidelines for the seismic design of oil and gas pipeline systems, American Society of Civil Engineers, Committee on Gas Liquid Fuel Lifelines

Bransby M, Nahas E, Turner E. and Davies M (2007) "The interaction of reverse faults with flexible continuous pipelines," *International Journal of Physical Modelling in Geotechnics*, 7: 25-40

Ha D, Abdoun TH, O'Rourke MJ, Symans MD, O'Rourke TD, Palmer MC and Stewart HE (2008) "Buried high-density polyethylene pipelines subjected to normal and strike-slip faulting - a centrifuge investigation," *Canadian Geotechnical Journal*, 45(12): 1733-1742

Janbu N (1963) "Soil compressibility as determined by oedometer and triaxial tests", *Proceedings of the European Conference on Soil Mechanics and Foundation Engineering*, Wissbaden, Germany, 19-25

Karamitros DK, Bouckovalas GD and Kouretzis GP (2007) "Stress analysis of buried steel pipelines at strike-slip fault crossings," *Soil Dynamics and Earthquake Engineering*, 27(3): 200-211

Karimian SA (2006) Response of buried steel pipelines subjected to longitudinal and transverse ground movement, Ph.D. Thesis, Department of Civil Engineering, The University of British Columbia, Vancouver, B.C., Canada

Kennedy RP, Chow A and Williamson R (1977) "Fault movement effects on buried oil pipeline," *Journal of Transportation Engineering,* 103(5): 617-633

Moore ID (2013) "Large-scale laboratory experiments to advance the design and performance of buried pipe infrastructure", *Proceedings of Keynote, ICPTT 2012: Better Pipeline Infrastructure for a Better Life*, Wuhan, China, 805-815

Moore ID and Hu FP (1996) "Linear viscoelastic modelling of profiled high density polyethylene pipe," *Canadian Journal of Civil Engineering*, 23: 395-407

Muir Wood D (2002) "Some observations of volumetric instabilities in soils" *International Journal of Solids and Structures*, 39(13): 3429-3449

Newmark NM and Hall WJ (1975) "Pipeline design to resist large fault displacement", *Proceedings of the U.S. National Conference on Earthquake Engineering*, Ann Arbor, MI

Ni P, Moore ID and Take WA (2014) "Numerical modeling of normal fault-pipeline interaction and comparison with centrifuge tests," to be submitted to *Soil Dynamics and Earthquake Engineering*

O'Rourke MJ and Liu X (1999) Response of buried pipelines subject to earthquake effects, Monograph No. 3, Multidisciplinary Center for Earthquake Engineering Research, University at Buffalo, US

Robert DJ (2010) Soil-pipeline interaction in unsaturated soils, Ph.D. thesis, University of Cambridge, UK

Saiyar M (2011) Behaviour of buried pipelines subject to normal faulting, Ph.D. Thesis, Queen's University, Kingston, ON, Canada

Selig ET (1990) "Soil properties for plastic pipe installations", Buried Plastic Pipe Technology, Edited by G.S. Buczala, Cassady, M.J., Philadephia, PA, US, 141-158

Sim WW, Towhata I, Yamada S and Moinet GJM (2012) "Shaking table tests modelling small diameter pipes crossing a vertical fault," *Soil Dynamics and Earthquake Engineering*, 35: 59-71

Vazouras P, Karamanos SA and Dakoulas P (2010) "Finite element analysis of buried steel pipelines under strike-slip fault displacements," *Soil Dynamics and Earthquake Engineering*, 30(11): 1361-1376

Weerasekara L and Wijewickreme D (2008) "Mobilization of soil loads on buried, polyethylene natural gas pipelines subject to relative axial displacements," *Canadian Geotechnical Journal*, 45(9): 1237-1249

Xie X, Symans MD, O'Rourke MJ, Abdoun TH, O'Rourke TD, Palmer MC and Stewart HE (2013) "Numerical modeling of buried HDPE pipelines subjected to normal faulting: a case study," *Earthquake Spectra*, 29(2): 609-632

Yimsiri S, Soga K, Yoshizaki K, Dasari GR and O'Rourke TD (2004) "Lateral and upward soil-pipeline interactions in sand for deep embedment conditions," *Journal of Geotechnical and Geoenvironmental Engineering*, 130(8): 830-842